

Spurious ‘active longitudes’ in parametric models of heavily spotted eclipsing binaries

S.V. Jeffers¹

¹School of Physics and Astronomy, University of St Andrews, North Haugh, St Andrews, Fife KY16 9SS, U.K.

ABSTRACT

In this paper, size distributions of starspots extrapolated from the case of the Sun, are modelled on the eclipsing binary SV Cam to synthesise images of stellar photospheres with high spot filling factors. These spot distributions pepper the primary’s surface with spots, many of which are below the resolution capabilities of eclipse mapping and Doppler imaging techniques. The lightcurves resulting from these modelled distributions are used to determine the limitations of image reconstruction from photometric data. Surface brightness distributions reconstructed from these lightcurves show distinctive spots on the primary star at its quadrature points. It is concluded that two-spot modelling or chi-squared minimisation techniques are more susceptible to spurious structures being generated by systematic errors, arising from incorrect assumptions about photospheric surface brightness, than simple Fourier analysis of the light-curves.

Key words:

stars: activity, spots, imaging binaries: eclipsing

1 INTRODUCTION

Doppler imaging has shown that rapidly rotating RS CVn binary systems, such as SV Cam (F9 V + K4 V, $P_{rot}=0.59$ d) frequently show spots at high and polar latitudes. A successful theoretical model of the formation of polar spots assumes that magnetic flux from decaying active regions is swept toward the poles by meridional flows (Schrijver & Title 2001). However, in order to produce polar spots bipolar active regions have to emerge at a rate approximately 30 times faster than in the case of the Sun, implying that the photospheres of active stars should be peppered with a large number of small spots.

Jeffers et al.(2005) used spectrophotometric data from the *Space Telescope Imaging Spectrograph* on board the Hubble Space Telescope to eclipse map the inner face of the primary of the RS CVn SV Cam. These observations and the HIPPARCOS parallax showed that the surface flux in the eclipsed low latitude region is approximately 30% lower than computed from the best fitting PHOENIX Allard et al. (2000) model atmosphere. This flux deficit can only be accounted for if approximately 28% of the primary’s surface is peppered with dark spots too small to be resolved through eclipse-mapping techniques where the resolution limit is approximately 1.5 degrees.

This paper extends the work of Jeffers et al. (2005) by applying the extrapolated solar spot size distribution of Solanki (1999) to a hypothetically immaculate primary star of SV Cam. We determine how different degrees of spot coverage influence the shape of the binary system’s lightcurve, and how accurately these lightcurves are reconstructed into surface brightness distributions

using the Maximum Entropy (Max Ent) eclipse mapping technique (Collier Cameron 1997; Collier Cameron & Hilditch 1997).

2 MODELLED DATA

2.1 Size distribution of spots on active stars

The variable nature of the spot coverage of active stars makes the quantification of their spot size distribution an intriguing problem. In the case of the Sun, the spot size distribution has been determined by Bogdan et al. (1988) from direct observations taken from the Mount Wilson white-light plate collection covering the period 1917-1982. When plotted on a log-log scale the size distribution of sunspots is parabolic, implying a two-parameter log-normal distribution, which cannot be represented by a single parameter distribution such as a power law. Following Bogdan et al. (1988) the number of sunspots, N , as a function of the solar surface area, A , is equated as,

$$\frac{dN}{dA} = \left(\frac{dN}{dA} \right)_{max} \exp \left(-\frac{(\ln A - \ln \langle A \rangle)^2}{2 \ln \sigma_A} \right) \quad (1)$$

where the constants $\langle A \rangle$ and σ_A are the mean and geometric standard deviation of the log-normal distribution, and $\left(\frac{dN}{dA} \right)_{max}$ the maximum value reached by the distribution. For the case of the Sun, these values are tabulated in Table 1 where set 1 is for an inactive Sun and set 2 is for an active Sun.

The extrapolation of the solar spot size distribution to active stars can be represented by different extrapolations e.g. Solanki

Set	1	2	3	4	5	6	7
Spot Coverage		0.3%	1.6%	6.1%	18%	48%	100%
σ_A	3.8	5.0	6.8	9.2	12.2	15.8	20.0
$(dN/dA)_{max}$	5	25	65	125	205	305	425
$A_{spot,tot} (\times 10^{-6})$	320	3000	16000	61000	186000	484000	10^6
$A_{max} (A_*)$	200	400	1000	3000	6000	10000	10000
Solar:	min	max					

Table 1. Tabulation of the input parameters to the log-normal size distribution of star spots, equation 1. The parameters derived by Bogdan et al. (1988) for the Sun are data sets 1&2, and those calculated by Solanki (1999) for active stars are data sets 3-7.

(1999) and Solanki & Unruh (2004). As long as the size distribution shows many sub-resolution spot that are not clumped together, the exact representation of the extrapolated size distribution is of minor importance. The extrapolation of Solanki (1999) is used, which is determined by analysing how the observable parameters of the log normal distribution, $(dN/dA)_{max}$, $\langle A \rangle$, and σ_A , change with increasing magnetic activity. The extrapolated size distributions cover a range of degrees of spottedness, from the one at solar minimum to a hypothetically completely spotted star. As adopted in the Solanki (1999) model, the penumbral diameter is included in the spot area (in the umbral to penumbral area ratio of 1:3) and is assumed to be independent of spot size. In all cases the minimum spot area is $1.5 \times 10^{-6} A_\odot$, where A_\odot is the surface area of the visible solar hemisphere. The input parameters for the log-normal distributions of Bogdan et al. (1988) and Solanki (1999) are tabulated in Table 1: sets 1 and 2 are for the inactive and active Sun, and sets 3 to 7 correspond to active stars with a spot coverage of 1.8%, 6.1%, 18%, 48% and 100% of their surface.

2.2 Generation of randomly distributed spots

The binary eclipse mapping code DoTS (Collier Cameron 1997) was used to synthesise spot maps which follow a log-normal size distributions on the surface of an immaculate SV Cam's primary (primary: $R_1=1.24R_\odot$, $T_{eff}=6038$ K, secondary: $R_2=0.79R_\odot$, $T_{eff}=4804$ K) to incorporate the surface geometry and radial velocity variations of tidally distorted close binary stars. The input parameters to DoTS for modelling spots are, where x is the output from the random number generator ($0 \leq x \leq 1$);

- (i) **longitude:** randomly distributed between 0° & 360°
- (ii) **latitude:** $-\frac{\pi}{2} < \theta < \frac{\pi}{2}$, following $\theta = \arcsin(2x + 1)$ with $0 \leq x \leq 1$, to eliminate an artificial concentration of spots at the pole
- (iii) **spot radius:** computed using the previously described log-normal distribution as tabulated in Table 1
- (iv) **spot brightness & spot sharpness:** modelled to obtain an umbral to penumbral ratio of 1:3.

2.3 Spot distributions

The spot distributions resulting from the size distributions given in Table 1 are shown on the left hand side of Figure 1 (sets 1 to 3) and in Figure 2 (sets 4 to 7). The degree of spottedness increases from the set at solar minimum (top of Figure 1) to the set with 100% spot coverage (bottom of Figure 2) to show the extreme effect of spot coverage. In this case, as the spot coverage fraction includes the spot's umbra + penumbra, the result is not a completely black star.

These modelled spot distributions were used to generate a synthetic lightcurve, comprising 500 points with uniform sampling and with random Gaussian noise (0.0004) added to match the photometric precision of our HST data. The central lightcurve wavelength, 4670Å, was also chosen to match that of our HST data.

3 SURFACE BRIGHTNESS IMAGE RECONSTRUCTION

The resulting lightcurve from the modelled distributions of spots, as described in the previous section, is used as input to DoTS to reconstruct the surface brightness distribution using the maximum entropy χ^2 minimisation method (Collier Cameron 1997).

3.1 System parameters

In the reconstruction of a surface brightness distribution of a binary star, it is imperative that the correct binary system parameters are used (Vincent et al. 1993). Incorrect binary system parameters lead to a poor fit of the photometric lightcurve and to the appearance of spurious spot features on the surface brightness image to compensate for this. In this work, the assumed spot temperature used is 1500 K cooler than the star's photospheric temperature. As the spot coverage increases, the surface brightness of the star will decrease compared to the star's photospheric brightness. This is particularly relevant for sets 4 to 7, where there is a high degree of spot coverage. In reconstructing the surface brightness distributions for each of these sets the photospheric temperature, the primary radius and the secondary radius are treated as an unknown parameters. The best fitting parameters are determined using a 'grid search' method that uses, as input to DoTS, a grid of: photospheric temperatures ranging from 5500 K to 6100 K at 25 K intervals; primary radius values ranging from 1.22 to 1.26 R_\odot and secondary radius values ranging from 0.77 to 0.81 R_\odot , both in 0.005 R_\odot intervals. For each set, the lowest χ^2 value is determined by the minimum of a quadratic fit to these values. The resulting best-fitting parameters are summarised in Table 2. These values are used as the photospheric temperature and radii for the reconstruction of the primary's surface brightness distribution.

3.2 Final image reconstruction

The images reconstructed for sets 4 to 7 are shown in Figure 2, however, the over-all spot coverage for sets 1 to 3 in Figure 1 was too small to be reconstructed. The photometric lightcurves for sets 1 to 3 are shown in the right-hand side of Figure 1. For sets 4 to 7, the fit to the photometric lightcurve and reconstructed surface brightness images are shown respectively in the centre and the right-hand side of Figure 2.

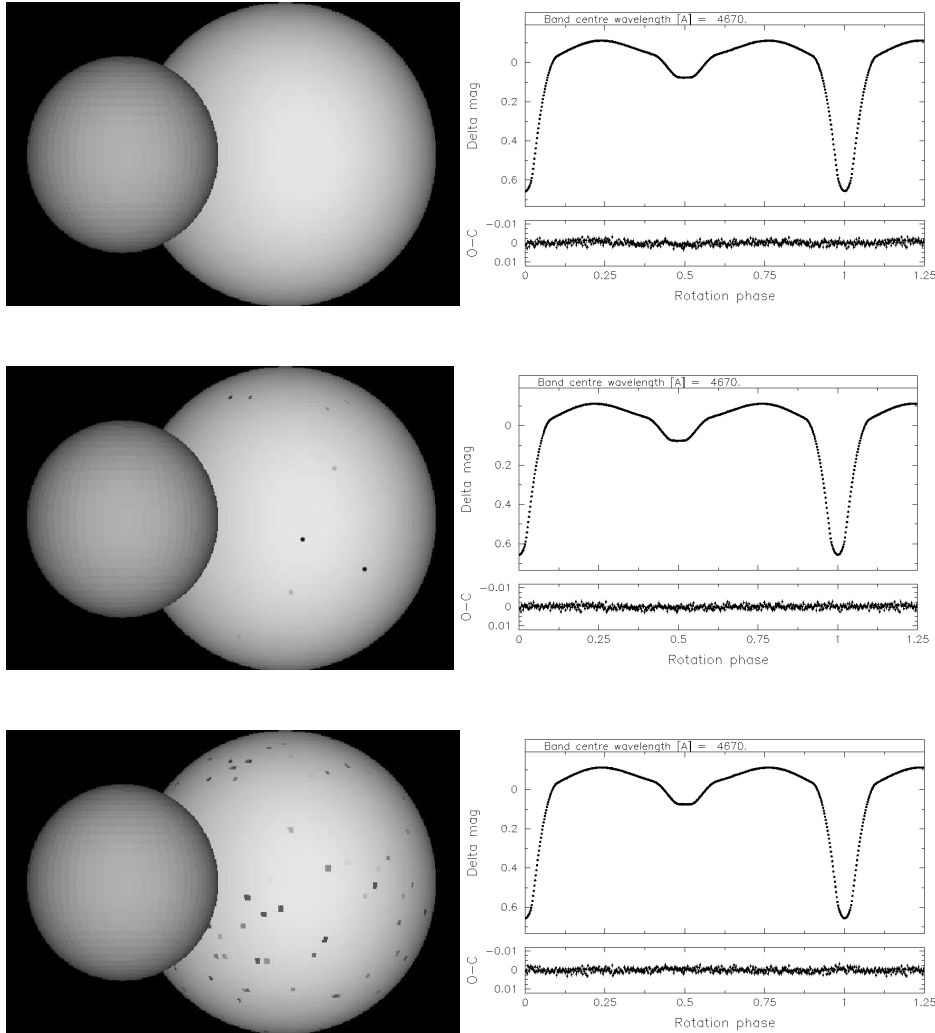


Figure 1. (left) The distribution of spot size distributions for sets 1 to 3. (right) The photometric lightcurve resulting from these spot distributions and the Max Ent model fit to these lightcurves. The Observed minus Computed lightcurves are plotted at the bottom of each lightcurve. It was not possible to reconstruct surface brightness distributions for these three sets as the spot coverage is too low to be recovered using eclipse-mapping.

Set	Primary Temperature (K)	R_{pri}/R_{\odot}	R_{sec}/R_{\odot}
initial	6038	1.25	0.81
4	6026 ± 40	1.230 ± 0.003	0.792 ± 0.003
5	5948 ± 71	1.248 ± 0.002	0.804 ± 0.003
6	5849 ± 53	1.251 ± 0.002	0.782 ± 0.004
7	5760 ± 45	1.252 ± 0.003	0.773 ± 0.005

Table 2. Best fitting binary system parameters for the size distribution sets 4 to 7 in Table 1

What is distinctive about these plots are the spot features at the quadrature points (90° and 270°). These spot features are not artifacts of the maximum entropy reconstruction, but occur as a

consequence of the χ^2 minimisation technique. If a star is peppered with small unresolvable spots, the effect on the star’s lightcurve will be to reduce the depth of the primary eclipse. To fit this with χ^2 minimisation it is necessary to increase the level of the whole computed lightcurve to fit the reduced primary eclipse depth. The difference in light at the quadrature points can only be accounted for by placing large spurious spots at these longitudes.

For sets 4 and 5, the spot feature at 270° longitude is fainter than the spot feature at 90° longitude as there is a higher degree of spot coverage at the first quadrature than at the second. In the reconstructed surface brightness distributions, the spots at 0° longitude result from the total spot coverage between second and third contact, i.e. during primary eclipse, while the spots at 180° longi-

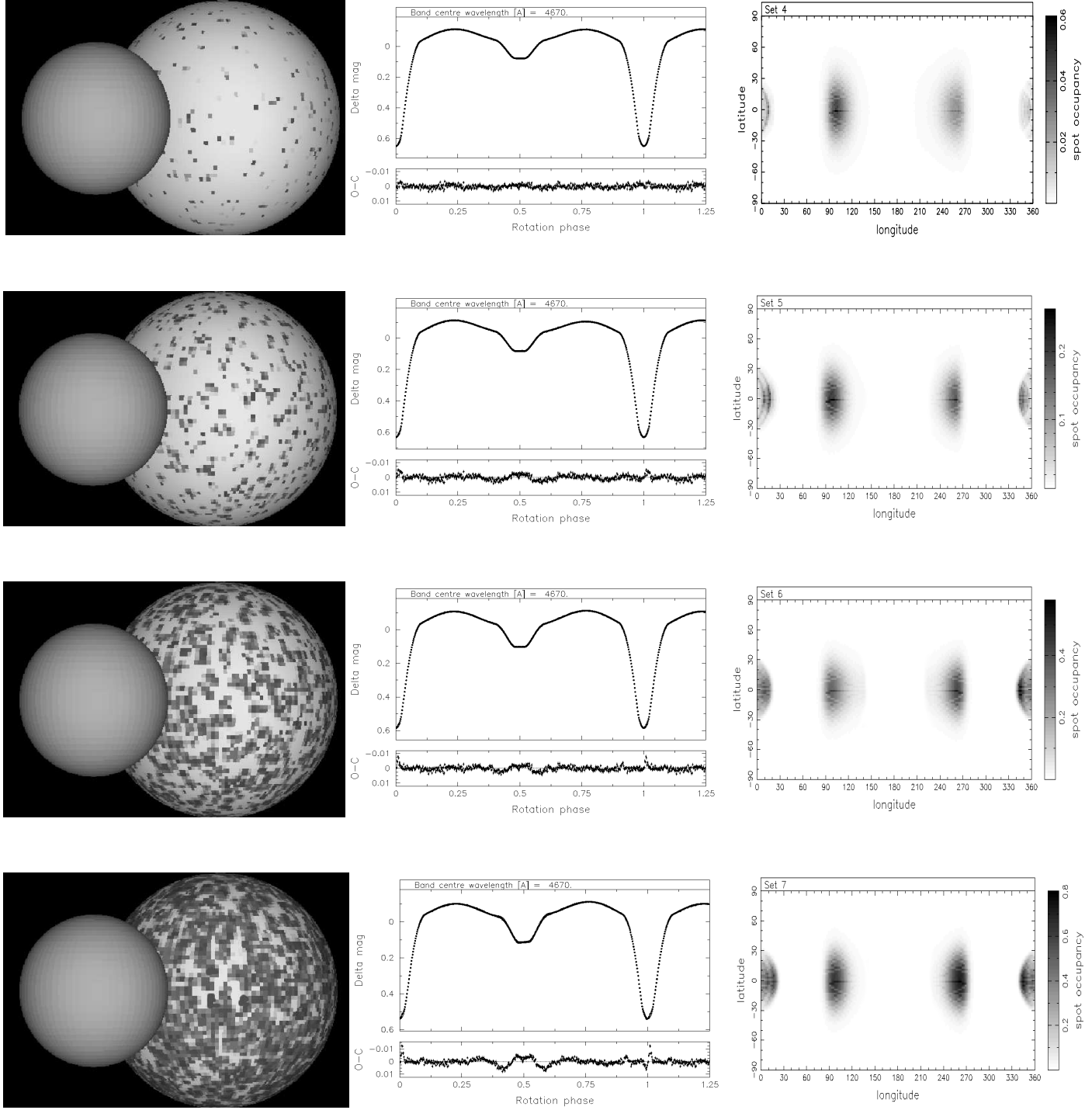


Figure 2. (left) The modelled distribution of spots for sets 4 (top) to 7 (bottom). (centre) The photometric lightcurve resulting from these spot distributions and the Max Ent model fit to these lightcurves. The Observed minus Computed lightcurves are plotted at the bottom of each lightcurve. (right) The surface brightness distribution that are reconstructed using the Max Ent eclipse-mapping technique, where phase runs in reverse to longitude. Note the large spurious spots at the quadrature points.

tude result from spots on the primary star visible during secondary eclipse.

4 DISCUSSION

Size distributions of starspots extrapolated from the case of the Sun (Solanki 1999), have been modelled on the eclipsing binary SV Cam to synthesise images of stellar photospheres with high spot filling factors. The lightcurves resulting from the extrapolated spot distributions were used as input to the Max Ent eclipse-mapping code DoTS. The resulting surface brightness distributions, with distinctive spot features at the quadrature points (90° and 270°), bear little resemblance to the input distribution of spots. These spurious spots at the quadrature points (90° and 270°) are not artifacts of the eclipse mapping technique, but a consequence of the χ^2 minimisation method.

The presence of spots over a large fraction of the stellar surface influences the shape of the lightcurve and consequently the derived stellar parameters. The peppering of the stellar surface with small unresolvable spots decreases the depth of the primary eclipse, resulting in a lower photospheric temperature of the primary star and a corresponding change in the radii of both binary components. The change in the binary system parameters (cf Table 2) shows how the degree of spottedness affects the determination of the correct photospheric temperature and radii when only photometric observations are used.

Spot features occurring at the quadrature points are commonly reconstructed features of RS CVn binaries and typically referred to as ‘active longitudes’. They are interpreted as being the preferred longitude of emergence of magnetic flux. These features have been observed on numerous short-period active RS CVn binary stars such as EI Eri, II Peg, σ Gem, HR 7275, AR Lac, SZ Psc, HK Lac (Berdyugina & Tuominen 1998; Lanza et al. 1998; Lanza et al. 2001; Jetsu 1996; Henry et al. 1995; Olah et al. 1991). In these cases, however, the ‘active longitudes’ have been determined through a Fourier analysis of the lightcurves and clearly show migration over several epochs. The fixed longitudes found in this work would indicate that is unlikely that migration could be reproduced by random distributions of spots.

Another approach for the reconstruction of a surface brightness distribution is the ‘two-spot’ model. The ‘two-spot’ model can account for the light variations of chromospherically active stars and examples of this model applied to SV Cam can be found in: Zboril & Djurašević (2003), Albayrak et al. (2001), Kjurkchieva et al. (2000), Djurasevic (1998), Patkos & Hempelmann (1994), Budding & Zeilik (1987) and Zelik et al. (1988). However Doppler images of chromospherically active RS CVn stars (e.g. Petit et al. (2002)) show more complicated distributions of spots than can be reconstructed with the ‘two-spot’ model. To investigate the reliability of the ‘two-spot’ model Eaton et al. (1996) modelled up to 40 randomly distributed spots on a single star, and found that they could reproduce ‘two-spot’ solutions similar to those reconstructed for actual stars. We have extended the work of Eaton et al. (1996) to show that the flux deficit caused by the presence of many sub resolution spots can be modelled by two spurious spots at the quadrature points.

It is concluded that ‘two-spot’ modelling or chi-squared minimisation techniques are more susceptible to spurious structures being generated by systematic errors, arising from incorrect assumptions about photospheric surface brightness, than simple Fourier analysis of the light-curves.

ACKNOWLEDGMENTS

The author would like to thank A. Collier Cameron, and V. Holzwarth for useful discussions, and acknowledges support from a PPARC research studentship and a scholarship from the University of St Andrews.

REFERENCES

Albayrak B., Demircan O., Djurašević G., Erkapić S., Ak H., 2001, A&A, 376, 158
 Allard F., Hauschildt P. H., Schweitzer A., 2000, ApJ, 539, 366
 Berdyugina S. V., Tuominen I., 1998, A&A, 336, L25
 Bogdan T., Gilman P., Lerche I., Howard R., 1988, ApJ, 327, 451
 Budding E., Zeilik M., 1987, ApJ, 319, 827
 Collier Cameron A., 1997, MNRAS, 287, 556
 Collier Cameron A., Hilditch R. W., 1997, MNRAS, 287, 567
 Djurasevic G., 1998, A&A, 127, 233
 Eaton J. A., Henry G. W., Fekel F. C., 1996, ApJ, 462, 888
 Henry G. W., Eaton J. A., Hamer J., Hall D. S., 1995, ApJS, 97, 513
 Jeffers S. V., Collier Cameron A., Barnes J. R., Aufdenburg J. P., Hussain G. A. J., 2004, submitted to Astrophysical Journal
 Jetsu L., 1996, A&A, 314, 153
 Kjurkchieva D., Marchev D., Ogloza W., 2000, Acta Astronomica, 50, 517
 Lanza A. F., Catalano S., Cutispoto G., Pagano I., Rodono M., 1998, A&A, 332, 541
 Lanza A. F., Rodonò M., Mazzola L., Messina S., 2001, A&A, 376, 1011
 Olah K., Hall D. S., Henry G. W., 1991, A&A, 251, 531
 Patkos L., Hempelmann A., 1994, A&A, 292, 119
 Petit P., Donati J.-F., Collier Cameron A., 2002, MNRAS, 334, 374
 Schrijver C. J., Title A. M., 2001, ApJ, 551, 1099
 Solanki S. K., 1999, in ASP Conf. Ser. 158: Solar and Stellar Activity: Similarities and Differences Spots and Plages: the Solar Perspective. p. 109
 Solanki S. K., Unruh Y. C., 2004, MNRAS, 348, 307
 Vincent A., Piskunov N. E., Tuominen I., 1993, A&A, 278, 523
 Zboril M., Djurašević G., 2003, A&A, 406, 193
 Zelik M., de Blasi C., Rhodes M., Budding E., 1988, ApJ, 332, 293

This paper has been typeset from a \TeX / \LaTeX file prepared by the author.